Journal of Alloys and Compounds 509 (2011) 3363–3366

Contents lists available at ScienceDirect

Journal of Alloys and Compounds

journal homepage: www.elsevier.com/locate/jallcom

Broadband UV excitable near-infrared downconversion luminescence in Eu^{2+}/Yb^{3+}:CaF_2 nanocrystals embedded glass ceramics

Hang Lin, Daqin Chen, Yunlong Yu, Zhifa Shan, Ping Huang, Anping Yang, Yuansheng Wang*

State Key Laboratory of Structural Chemistry, Fujian Institute of Research on the Structure of Matter, Chinese Academy of Sciences, Graduate University of Chinese Academy of Sciences, Fuzhou, Fujian 350002, China

ARTICLE INFO

Article history:
Received 25 September 2010
Received in revised form 9 December 2010
Accepted 9 December 2010
Available online 16 December 2010

Keywords:
Glass ceramics
Nanocomposites
Downconversion
Spectroscopy
Optical properties

ABSTRACT

Cooperative downconversion was realized in glass ceramics containing Eu^{2+}/Yb^{3+}:CaF_2 nanocrystals with Eu^{2+} greatly absorbing ultraviolet photons. Upon excitation of Eu^{2+} ions to the 5*d* level with an ultraviolet photon at 320 nm, emission of two near infrared photons at 976 nm of Yb^{3+} were achieved. The dependence of the visible and near-infrared emissions, decay lifetime, and quantum efficiency on the Yb^{3+} doping content has been investigated. The maximum energy transfer efficiency and the corresponding downconversion quantum efficiency were estimated to be 51% and 151%, respectively.

1. Introduction

Owning to the mismatch between the solar spectrum and the spectral response of crystal silicon (c-Si) solar cells, great parts of solar energy dissipated in photovoltaic PV module either by transmission or charge carriers thermalization [1]. Taking account of these energy loss, Queisser and Shockley have proposed that an upper theoretical limit for the energy efficiency of single p-n junction with energy band gap (Eg) of 1.1 eV is 30% [2]. Adapting the solar spectrum through downconversion (DC) would be an optimizing scheme to exceed the Queisser–Shockley limit [1,3], which based on the principle that DC phosphor could generate two or more low-energy photons after absorbing a high-energy photon. If conversion of an incident ultraviolet (UV)–visible photon into two near-infrared (NIR) photons is realized, the energy loss due to thermalization of the electron-hole pairs could be reduced [4,5]. Rare earth (RE) ions are optimal candidates for DC, thanking to their abundant energy levels. In recent years, some RE ions (Tb^{3+}/Yb^{3+} [6,7], Tm^{3+}/Yb^{3+} [8,9], Pr^{3+}/Yb^{3+} [1,10,11]) doped glass ceramics or nanocrystals have been intensively investigated. However, the low absorption cross-sections of these RE ions arising from parity-forbidden 4*f*–4*f* transitions inhibit them from absorbing a large part of solar radiation. In this case, Ce^{3+}/Yb^{3+} or Eu^{2+}/Yb^{3+} couples are good alternatives since Ce^{3+} and Eu^{2+} have strong *f*–*d* absorbing transitions in the desired spectral region [12]. The Ce^{3+}/Yb^{3+} based DC was firstly realized in borate glasses by Wang et al. [13], and Zhou et al. [14] initially observed DC in Eu^{2+}/Yb^{3+} co-doped borate glasses. It was confirmed that the cooperative DC mechanism based on one donor exciting two acceptors simultaneously is responsible for the energy transfer (ET) process from Ce^{3+} or Eu^{2+} to Yb^{3+}.

Transparent oxyfluoride glass ceramics (GC) are preferable hosts for DC [9,10], owning to their high mechanical and chemical stabilities of oxide matrix and low-phonon-energy environment of fluoride nanocrystals. When RE ions are partitioned into the precipitated fluoride nanocrystals, the efficiency of DC energy transfer between RE ions may increase due to the shortening distances between RE ions and the reducing probabilities of non-radiative relaxation. Especially, when Eu^{3+} is partitioned into MF_2 nanocrystals (M = Ca, Ba, Sr) in the glass ceramics [15,16], it will replace M^{2+} ion and is efficiently reduced to Eu^{2+} even in air atmosphere by charge compensation mechanism [17–20].

In this paper, transparent glass ceramics containing Eu^{2+}/Yb^{3+}:CaF_2 nanocrystals were successfully prepared by melt-quenching and subsequent heating. Remarkably, it is found that Eu^{2+} could absorb broadband light in the UV region and convert one UV photon to two NIR photons via cooperative energy transfer (CET) process.

2. Experimental details

The composition of the host precursor glass is $45SiO_2$–$25Al_2O_3$–$5CaCO_3$–$10NaF$–$15CaF_2$ (in mol%). RE dopants were introduced in the form of EuF_3 and YbF_3. The Eu^{3+} concentration was fixed to 0.5 mol%, while the Yb^{3+} one was set to be 0,

* Corresponding author. Tel.: +86 591 8370 5402; fax: +86 591 8370 5402.
E-mail address: yswang@fjirsm.ac.cn (Y. Wang).

0925-8388/$ – see front matter © 2010 Elsevier B.V. All rights reserved.
doi:10.1016/j.jallcom.2010.12.066

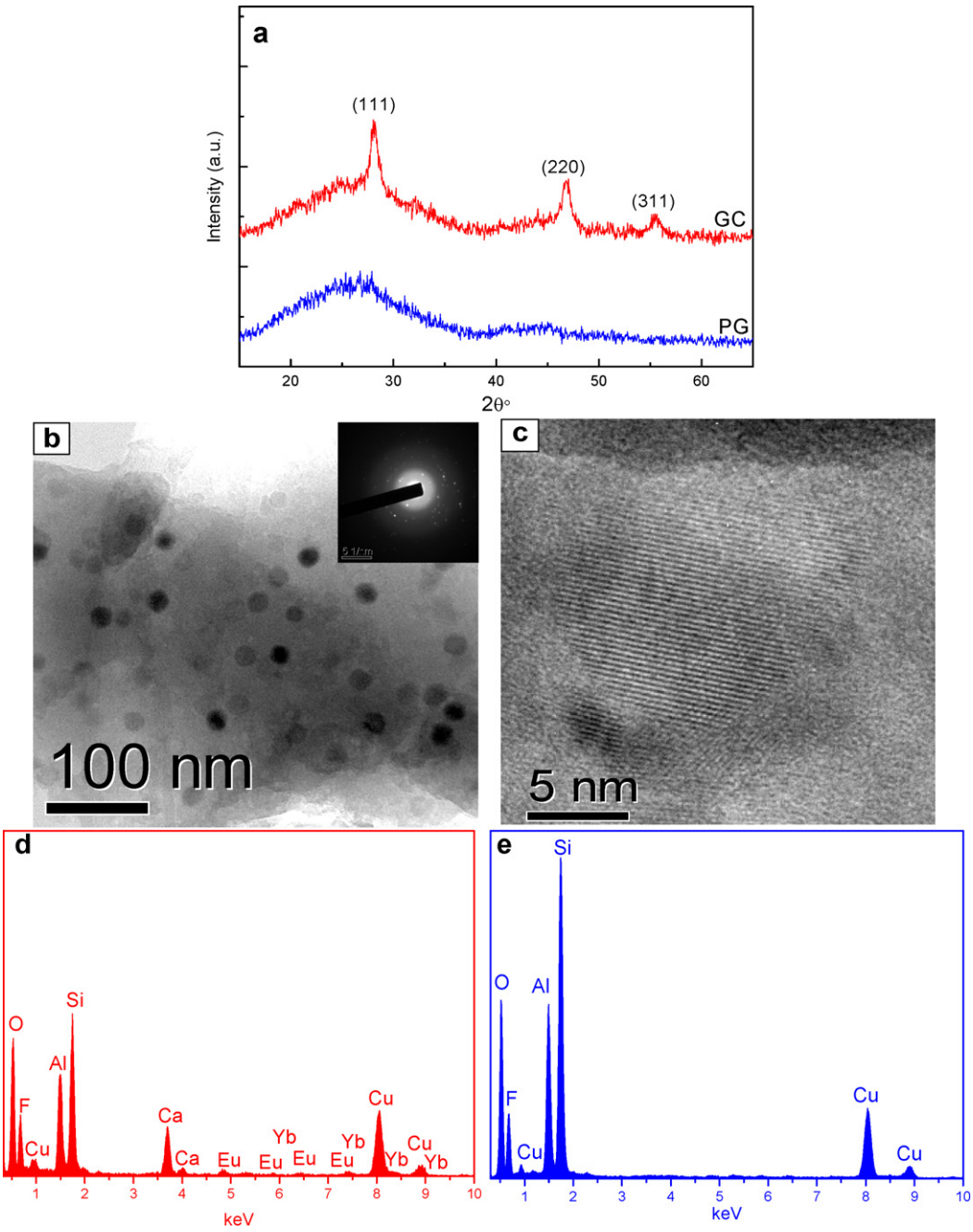

Fig. 1. (a) XRD curves of precursor glass (PG) and the corresponding glass ceramic (GC); (b) TEM micrograph of glass ceramic containing $0.5Eu^{2+}/0.2Yb^{3+}$:CaF_2, inset shows the selected area electron diffraction pattern; (c) HRTEM image of an individual nanocrystal; (d) EDS spectra taken from an individual nanocrystal and (e) from glass matrix in the glass ceramic containing CaF_2:$0.5Eu^{2+}/0.2Yb^{3+}$.

0.2, 1.0, and 2.0 mol%, respectively. For each batch, about 10 g of the mixed original materials were melted in a covered crucible in an air atmosphere at 1450 °C for 1.5 h, and then cast into a brass mold to form the precursor glass. In this procedure, carbon granules were used to supply the reducing atmosphere. The as-prepared samples were subsequently heat treated at 590 °C for 6 h to achieve glass ceramic through the desired crystallization.

X-ray diffraction (XRD) analysis was carried out with a powder diffractometer (DMAX2500 RIGAKU) using Cu Kα (λ = 0.154 nm) radiation to identify the phase structure. The microstructures of the samples were studied using a transmission electron microscope (TEM, JEM-2010) equipped with the energy dispersive X-ray spectroscopy (EDS) system. The emission and excitation spectra were recorded on an Edinburgh Instruments FLS920 spectrofluorometer equipped with a xenon lamp as excitation source. The fluorescence decay curves were recorded with a Near-infrared Photomultiplier Tube (R5509) excited by a nanosecond flash lamp. All the measurements were carried out at room temperature.

3. Results and discussion

XRD curve of the precursor glass exhibits the amorphous humps originating from the oxide glassy matrix, as shown in Fig. 1a, while XRD curve of the glass ceramic shows the characteristic sharp peaks of the crystalline phase which could be assigned to the orthorhombic CaF_2 (JCPDS 65-0535). Based on the peak widths, the mean size of the CaF_2 crystallites is evaluated to be 10 nm by Debye–Scherrer formula. By TEM observation shown in Fig. 1b, it is found that 9–12 nm sized CaF_2 nanoparticles distribute homogenously in the glass matrix, in good agreement with XRD result. Revealed by high resolution TEM (HRTEM) image, the CaF_2 nanoparticles exhibit good crystallinity, as displayed in Fig. 1c. In order to detect the

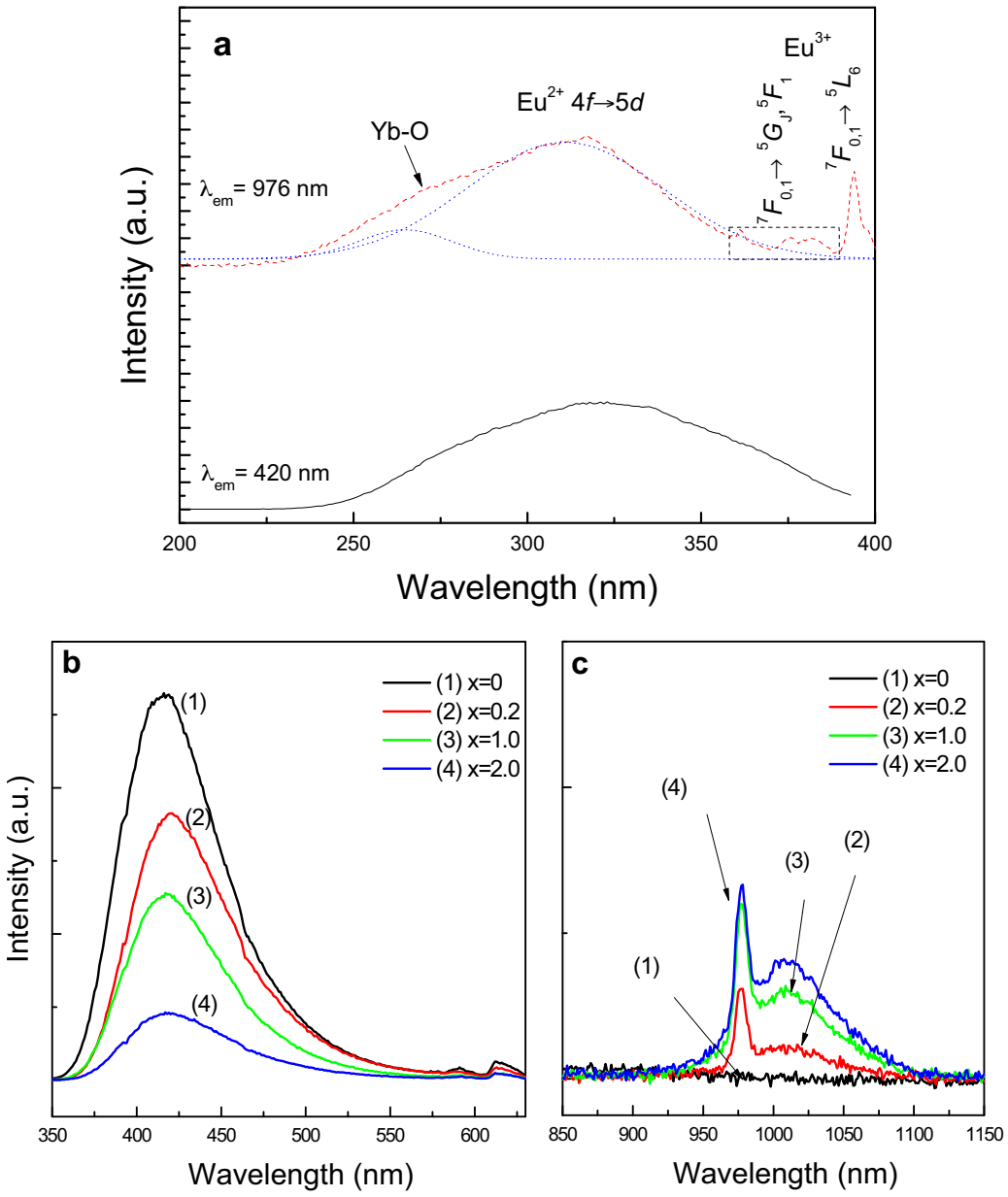

Fig. 2. (a) Photoluminescence excitation spectra of Eu^{2+}: $5d \rightarrow 4f$ emission (420 nm, black and solid) in Eu^{2+} single doped glass ceramic, and Yb^{3+}: $^2F_{5/2} \rightarrow {}^2F_{7/2}$ emission (976 nm, red and dashed) in glass ceramic containing $0.5Eu^{2+}/0.2Yb^{3+}$:CaF_2; the blue and dotted lines represent data fit using Gaussian function; (b) visible and (c) NIR photoluminescence spectra of glass ceramics with different Yb^{3+} concentrations (x%), excited at 320 nm. (For interpretation of the references to color in this figure legend, the reader is referred to the web version of the article.)

distribution of the doped RE ions, EDS spectra with nanosized electron probe were recorded. The spectrum from an individual CaF_2 nanocrystal (Fig. 1d) exhibits Ca, F, Yb, and Eu signals (the Al, Si, and O signals are attributed to the glass matrix surrounding the nanosized crystal, and the Cu peaks are originated from the copper grid supporting the TEM sample), while the spectrum from the glass matrix (Fig. 1e) exhibits no RE signals. This result implies that the doped RE ions concentrate mainly in the CaF_2 nanocrystals.

The excitation and emission spectra of Eu^{2+} single doped glass ceramic are shown in Fig. 2. Both spectra exhibit characteristic broadband absorption (ranging from 230 nm to 390 nm) and emission (centered at 420 nm) of Eu^{2+} ascribing to the allowed Eu^{2+}: $4f \leftrightarrow 5d$ transitions. As for the photoluminescence excitation spectra of the Eu^{2+}/Yb^{3+} co-doped samples shown in Fig. 2a, the broad spectral profile of the Yb^{3+} NIR emission at 976 nm is similar to the one of the Eu^{2+}: $4f \rightarrow 5d$ transition, indicating the energy transfer from Eu^{2+} to Yb^{3+}. A shoulder peak centering at 270 nm could be assigned to the O^{2-}–Yb^{3+} charge transfer [21], and it ends at 300 nm as revealed by the Gaussian deconvolution. Therefore, the influence of O^{2-}–Yb^{3+} charge transfer on the energy transfer from Eu^{2+} to Yb^{3+} would not be considered when excited at 320 nm. The peaks around 370 nm and 394 nm come from the Eu^{3+}: $^7F_{0,1} \rightarrow {}^5G_J$, $^5F_1$ and $^7F_{0,1} \rightarrow {}^5L_6$ transitions. However, as proposed by Zhou [14], there is no apparent impact of Eu^{3+} ions on the IR luminescence of Yb^{3+} ions when excited at 320 nm. Considering that the Eu^{2+} $5d$ emission is located at approximately twice the energy of the Yb^{3+} $^2F_{5/2}$ one, and there is no energy level higher than $^2F_{5/2}$ for Yb^{3+}, the most possible energy transfer route would be Eu^{2+}: $5d \rightarrow Yb^{3+}$: $^2F_{5/2} + Yb^{3+}$: $^2F_{5/2}$. The corresponding emission spectra excited at 320 nm are shown in Fig. 2b and c. It is observed that, with increase of Yb^{3+} concentration, the emission intensity of Eu^{2+} at 420 nm decreases rapidly, while that of Yb^{3+} at 976 nm enhances gradually, which fur-

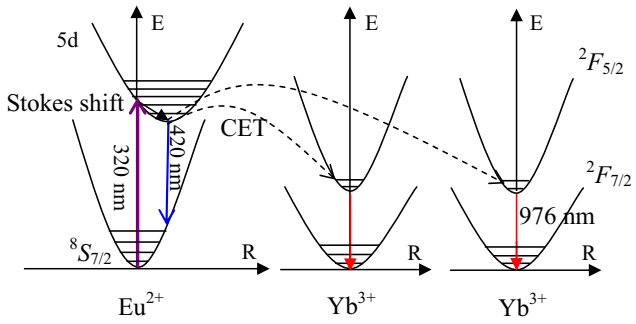

Fig. 3. Configuration coordinate model of energy transfer from Eu^{2+} to Yb^{3+}.

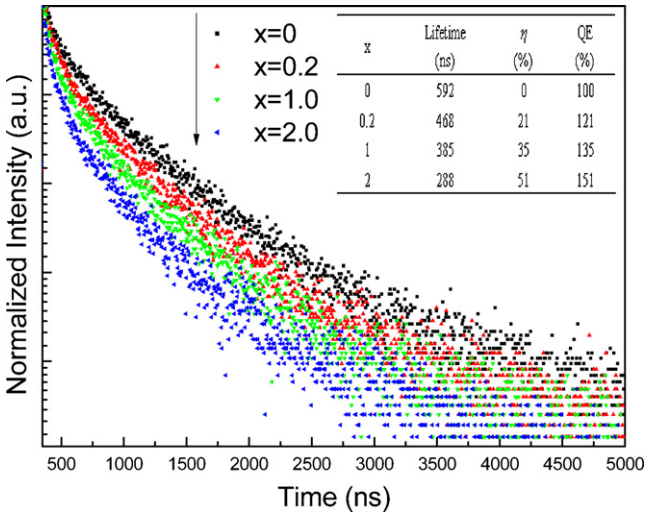

x	Lifetime (ns)	η (%)	QE (%)
0	592	0	100
0.2	468	21	121
1	385	35	135
2	288	51	151

Fig. 4. Decay curves of the Eu^{2+}: $5d \rightarrow 4f$ transition in the glass ceramics with different Yb^{3+} concentrations (x%), under 320 nm excitation; inset shows the dependences of decay lifetime, ETE, and QE on the Yb^{3+} concentration.

ther confirms the occurrence of energy transfer from Eu^{2+} to Yb^{3+}. The cooperative energy transfer (CET) process from Eu^{2+} to Yb^{3+} is depicted in Fig. 3, which demonstrates that the absorption of one incident UV photon results in the generation of two NIR photons.

The decay curves of the Eu^{2+} $5d \rightarrow 4f$ emissions at 420 nm for the glass ceramics with different Yb^{3+} concentrations of 0, 0.2, 1.0, and 2.0 mol% respectively are plotted in Fig. 4. The effective experimental lifetime (τ_{eff}) was evaluated by $\tau_{eff} = \int I(t)\,dt/I_p$, where $I(t)$ represents the luminescence intensity at time t after the cutoff of the excitation light, and I_p is the peak intensity in the decay curve. The obtained lifetime, as listed in the inset of Fig. 4, exhibits a rapid decreasing trend with increasing of Yb^{3+} concentration, which could be explained by the introduction of an extra relaxation pathway (CET from Eu^{2+}: $5d$ to Yb^{3+}: $^2F_{5/2}$). The energy transfer efficiency (ETE, $\eta_{tr,x\%Yb}$) from Eu^{2+} to Yb^{3+} was calculated by

$$\eta_{tr,x\%Yb} = 1 - \frac{\int I_{x\%Yb}\,dt}{\int I_{0\%Yb}\,dt} \quad (1)$$

to be 21%, 35%, and 51% for the samples with increasing Yb^{3+} concentration of 0.2, 1.0 and 2.0 mol%, respectively. The total quantum efficiency (QE), defined as the ratio of the number of photons emitted to the number of photons absorbed, could be estimated by the following equation assuming that all the excited Yb^{3+} ions decay radiatively ($\eta_{rYb} = 1$) [22]:

$$\eta_{x\%Yb} = \eta_{rEu}(1 - \eta_{tr,x\%Yb}) + 2\eta_{tr,x\%Yb} \quad (2)$$

Under the assumption that all the residual excited Eu^{2+} ions decays radiatively ($\eta_{rEu} = 1$), the theoretical DC QE for the 0.2, 1.0 and 2.0 mol% Yb^{3+} doped samples are determined to be 121%, 135% and 151%, respectively.

4. Conclusions

In summary, the Eu^{2+}/Yb^{3+} co-doped glass ceramics containing CaF_2 nanocrystals were developed. It was experimentally evidenced that two Yb^{3+} NIR photons emitted at 976 nm after absorbing an incident UV photon by Eu^{2+}. The maximum theoretical quantum efficiency was evaluated to be 151%. Such material might act as a promising DC converter to enhance the efficiency of the silicon solar cell by utilizing the broadband absorption in the ultraviolet region.

Acknowledgements

This work was supported by the National Natural Science Foundation of China (10974201, 50902130), the Natural Science Foundation of Fujian Province (2009J05139) and State Key Laboratory of Optoelectronic Materials and Technologies (KF2008-ZD-05).

References

[1] B.M. van der Ende, L. Aarts, A. Meijerink, Adv. Mater. 21 (2009) 1–5.
[2] T. Trupke, M.A. Green, P. Wurfel, J. Appl. Phys. 92 (2002) 1668–1674.
[3] C. Strumpel, M. McCann, G. Beaucarne, V. Arkhipov, A. Slaoui, V. Svrcek, C. del Canizo, I. Tobias, Sol. Energy Mater. Sol. Cells 91 (2007) 238–249.
[4] B.S. Richards, Sol. Energy Mater. Sol. Cells 90 (2006) 1189–1207.
[5] B.S. Richards, Sol. Energy Mater. Sol. Cells 90 (2006) 2329–2337.
[6] Q.Y. Zhang, C.H. Yang, Z.H. Jiang, X.H. Ji, Appl. Phys. Lett. 90 (2007) 061914.
[7] D.Q. Chen, Y.L. Yu, Y.S. Wang, P. Huang, F.Y. Weng, J. Phys. Chem. C 113 (2009) 6406–6410.
[8] Q.Y. Zhang, G.F. Yang, Z.H. Jiang, Appl. Phys. Lett. 91 (2007) 051903.
[9] S. Ye, B. Zhu, J. Luo, J.X. Chen, G. Lakshminarayana, J.R. Qiu, Opt. Express 16 (2008) 8989–8994.
[10] D.Q. Chen, Y.S. Wang, Y.L. Yu, P. Huang, F.Y. Weng, Opt. Lett. 33 (2008) 1884–1886.
[11] Lakshminarayana, J.R. Qiu, J. Alloy Compd. 29 (2009) 582–589.
[12] B.M. van der Ende, L. Aarts, A. Meijerink, Phys. Chem. Chem. Phys. 11 (2009) 11081–11095.
[13] D.Q. Chen, Y.S. Wang, Y.L. Yu, P. Huang, F.Y. Weng, J. Appl. Phys. 104 (2008) 116105.
[14] J.J. Zhou, Y.X. Zhuang, S. Ye, Y. Teng, G. Lin, B. Zhu, J.H. Xie, J.R. Qiu, Appl. Phys. Lett. 95 (2009) 141101.
[15] Q. Luo, X.S. Qiao, X.P. Fan, S.Q. Liu, H. Yang, X.H. Zhang, J. Non-Crystal. Solids 354 (2008) 4691–4694.
[16] J. Fu, M. Kobayashi, S. Sugimoto, J.M. Parker, J. Am. Ceram. Soc. 92 (2009) 2119–2121.
[17] Z.W. Pei, Q. Su, J.Y. Zhang, J. Alloys Compd. 198 (1993) 51–53.
[18] H.Y. Wu, Y.H. Hu, Y.H. Wang, C.J. Fu, J. Alloys Compd. 497 (2010) 330–335.
[19] Z.H. Lian, J. Wang, Y.H. Lv, S.B. Wang, Q. Su, J. Alloys Compd. 430 (2007) 257–261.
[20] R.P. Yavetskiy, E.F. Dolzhenkova, A.V. Tolmachev, S.V. Parkhomenko, V.N. Baumer, A.L. Prosvirnin, J. Alloys Compd. 441 (2007) 202–205.
[21] E. Nakazawa, Chem. Phys. Lett. 56 (1978) 161–163.
[22] P. Vergeer, T.J.H. Vlugt, M.H.F. Kox, M.I. den Hertog, J.P.J.M. van der Eerden, A. Meijerink, Phys. Rev. B 71 (2005) 014119.